

**Table. S1** Concentration of endocytosis inhibitors and markers used in this study

Drug/ treatment	Final Conc.	Pathway targeted/marked	Mode of action
NAV2729	25uM (in vitro) 5mM (in vivo)	Arf1/Arf6	Blocks ARNO- and GEP100-mediated guanine nucleotide exchange on Arf6, and inhibits the activation of $\Delta 17$ Arf1 by BRAG2Sec7PH
5-(N-ethyl-N-isopropyl)-amiloride (EIPA)	21uM (in vitro) 5mM (in vivo)	Macropinocytosis	Inhibits Na <sup>+</sup> /H <sup>+</sup> exchange; may affect actin
Chlorpromazine (CPZ)	4ug/ml	CME	Translocate clathrin and AP2 from the cell surface to intracellular endosomes. Inhibits CIE in some cells
Methyl- $\beta$ -cyclodextrin (MBCD)	1mM	Lipid raft; CME; fluid phase endocytosis	Removes cholesterol from the plasma membrane
Tfn-AF647	25 $\mu$ g/ml	CME	
Dextran-AF647	4mg/ml	Macropinocytosis	
CTxB-AF647	10 $\mu$ g/ml	CIE, CvME	

Abbreviations: CIE, clathrin-independent endocytosis; CME, clathrin-mediated endocytosis; CvME, caveolae-mediated endocytosis.

**Table. S2** Particle size and zeta potential of Tat/pDNA/C16TAB nanoparticles

Formulation	N/P ratio	Size/nm	Zeta Potential/mV
Tat/pGL3/C16TAB	1	209 $\pm$ 0.8	+11 $\pm$ 4.7
	10	82 $\pm$ 6.0	+28 $\pm$ 5.9
Tat/TF/C16TAB	1	214 $\pm$ 2.3	+9 $\pm$ 2.2
	10	83 $\pm$ 9.1	+22 $\pm$ 6.4
Tat/DiYO-1-pGL3/C16TAB	1	301 $\pm$ 8.2	+18 $\pm$ 5.7
	10	109 $\pm$ 7.6	+31 $\pm$ 6.3
Tat/ DiYO-1-TF/C16TAB	1	350 $\pm$ 5.7	+20 $\pm$ 3.4
	10	112 $\pm$ 4.0	+36 $\pm$ 4.8
Tat/DiYO-3-pGL3/C16TAB	1	303 $\pm$ 9.0	+18 $\pm$ 4.2
	10	108 $\pm$ 5.3	+32 $\pm$ 5.5
Tat/ DiYO-3-TF/C16TAB	1	356 $\pm$ 9.0	+23 $\pm$ 8.4
	10	112 $\pm$ 6.3	+35 $\pm$ 5.1

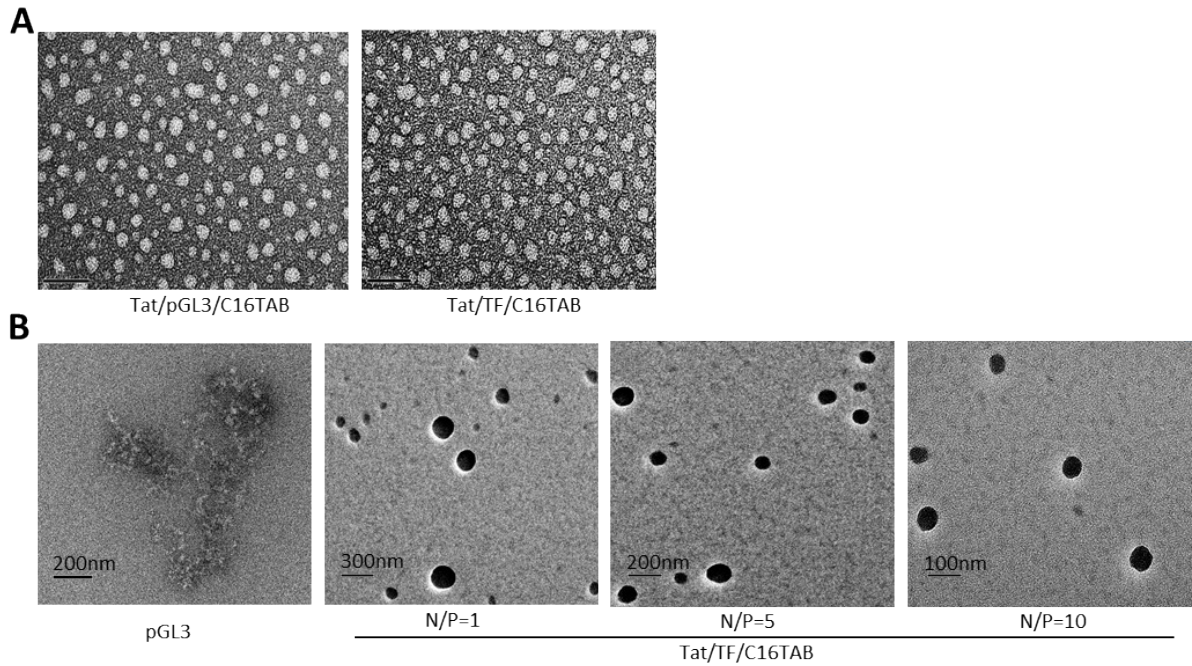


**Fig. S1** Representative TEM images of T-P-C nanoparticles. (A) No difference on the formulation of Tat/pDNA/C16TAB nanoparticles based on distinct plasmids. N/P=10. (B) Smaller size of T-P-C nanoparticles was formulated with increased N/P ratios.

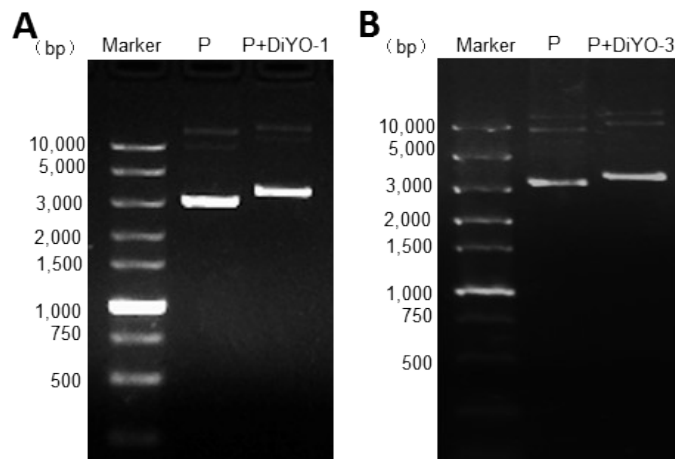


**Fig. S2** Labeling efficiency of DiYO-1 or DiYO-3 to pDNA is Similar. Agarose electrophoresis analysis of the mobility difference of pDNA (P: pGL3 plasmid) labeled with DiYO-1 (A) or DiYO-3 (B).

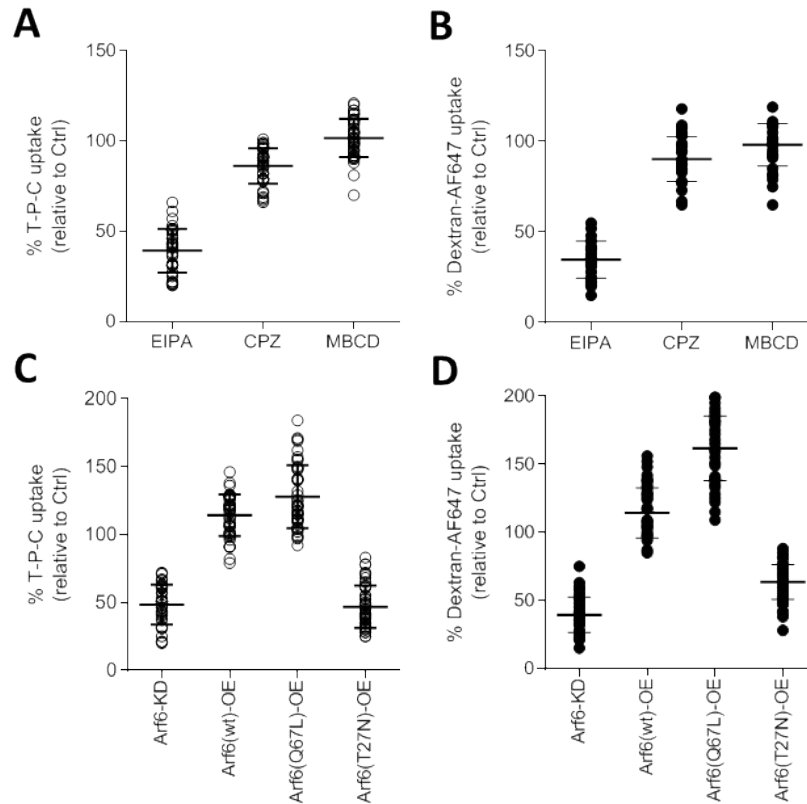


**Fig. S3** Scattershot depicts the uptake of indicating ligands in single cell populations. Uptake of DiYO-1-labeled T-P-C nanoparticles (A, C) and Dextran-AF647 (B, D) in inhibitor-treated (A, B) or Arf6-interfered (C, D) Skov3 cells were quantified by confocal imaging. At least 60 cells were counted for each treatment/transfection. Undisturbed Skov3 cells (Ctrl) were set as 100% for comparison.

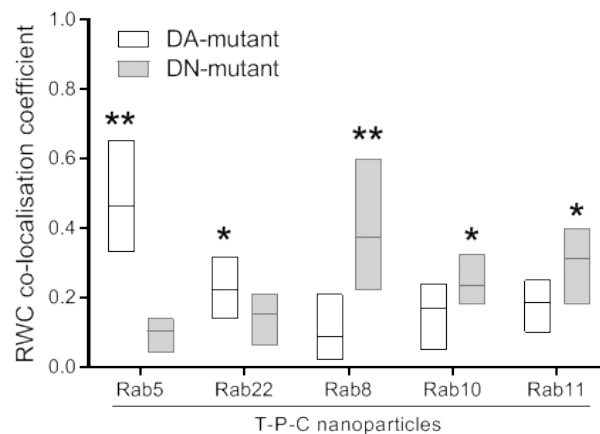


**Fig. S4** Co-localization analysis of T-P-C nanoparticles with expressed Rab mutants in cell populations. Box-and-whiskers plots depicting the co-localization of distinct Rab mutants with internalized T-P-C nanoparticles. Rank weighted coefficient (RWC) values were quantified.  $\geq 60$  cells were counted for each transfection.  $n = 3$ . Significant differences are shown.  $**p < 0.01$ ,  $*p < 0.05$ .

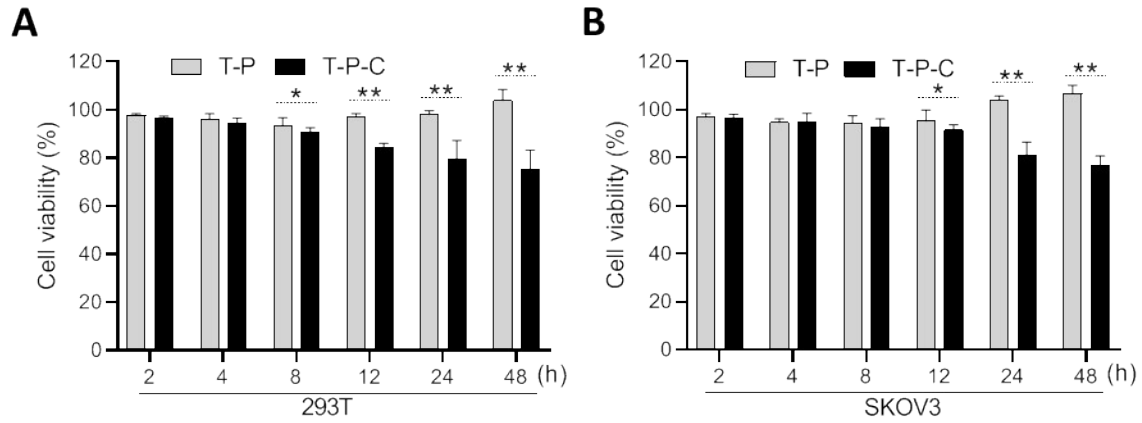


**Fig. S5** No cytotoxicity of T-P-C nanoparticles was observed after short-term incubation. Cytotoxicity of nanoparticles was checked by MTT assays on nontumorous 293T cells (A) and OC SKOV3 cells (B). Both T-P and T-P-C nanoparticles present no cytotoxicity after short time of incubation. A little cytotoxicity of T-P-C nanoparticles was observed after long time of incubation.  $n=3$ , \*\*  $P < 0.01$ , \*  $P < 0.05$ .

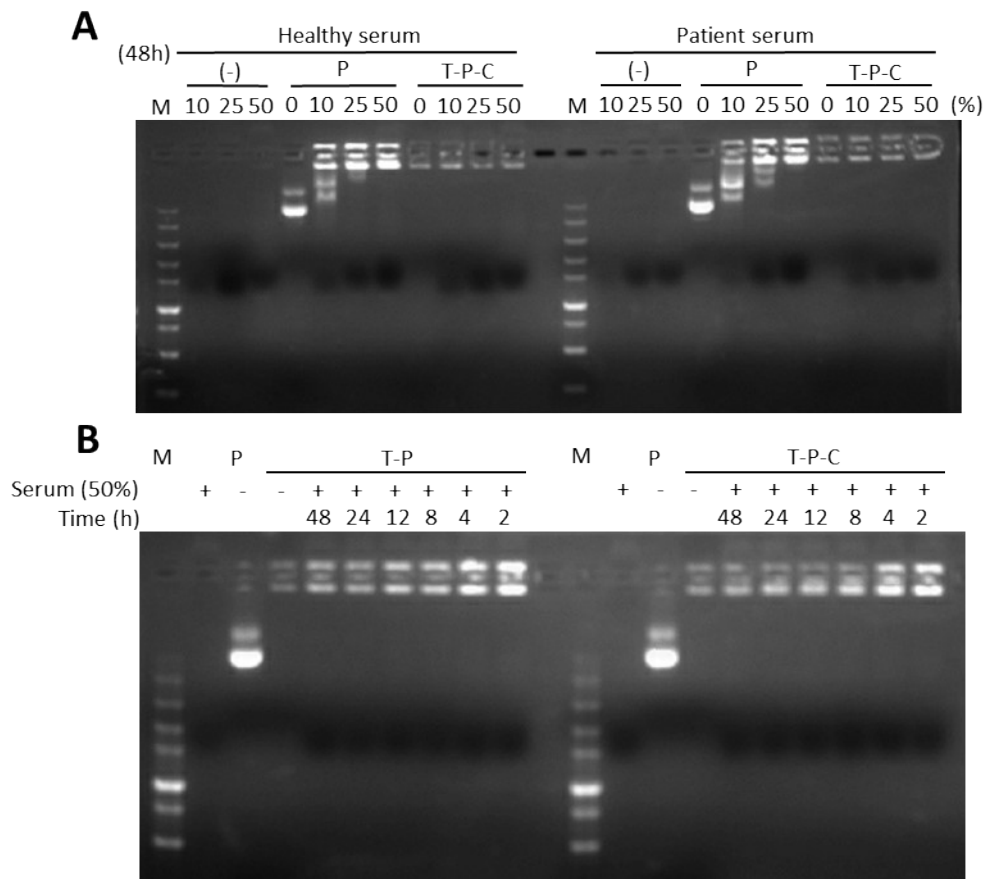


**Fig. S6** Characteristics of serum stability for T-P-C nanoparticles. (A) Agarose electrophoresis analysis of the stability of T-P-C nanoparticles incubated with healthy human serum and OC patient serum, respectively. P: TF pDNA. (-) only serum was loaded. (B) Time-course checking the stability of T-P and T-P-C nanoparticles by agarose electrophoresis analysis. N/P ratios=10. M: DNA ladder.

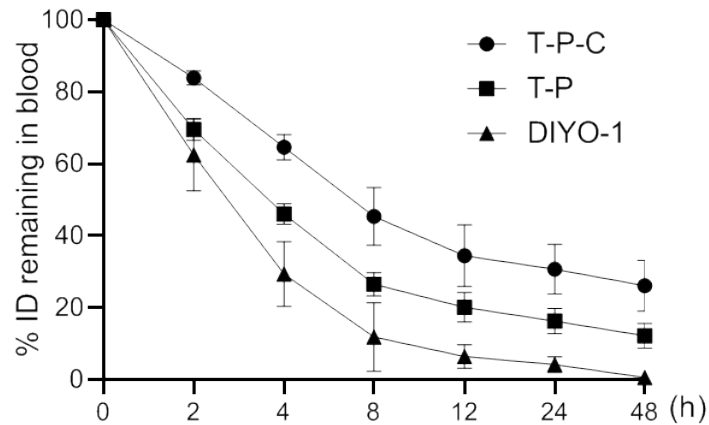


**Fig. S7** In vivo blood clearance rate of T-P-C nanoparticles. Blood clearance curves of T-P-C, T-P and free DIYO-1 in mice over 48h after intravenous injection. Balb/c-nu mice were divided into three groups (n=3 per group). DIYO-1-labelled nanoparticles (1 mg/kg. free dye at dose corresponded to its incorporating in nanoparticles) were injected via tail vein. Blood were collected at predetermined time points, and stored into tubes pretreated with 2 % EDTA solution. The DIYO-1 fluorescence intensity in blood samples was analyzed by fluorescence microplate reader. Data expressed as the percent of injected dose (% ID). The initial 5 min fluorescence intensity in the blood was taken as 100 %. Meanwhile, fluorescence intensity in blood from none-injected mice was regarded as background signal.

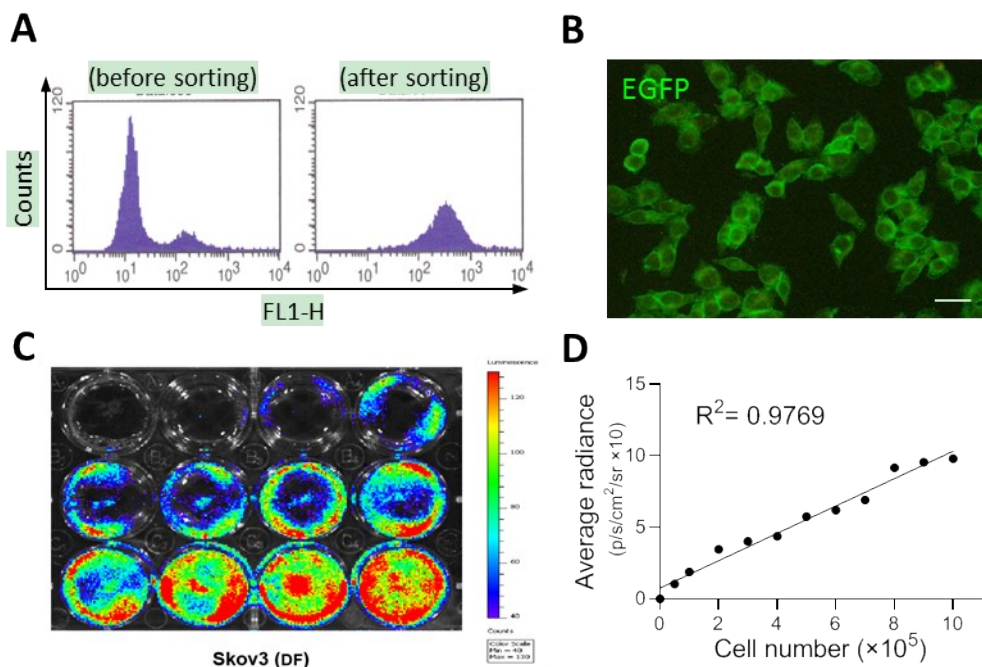


**Fig. S8** Identification of lentivirus-transduced Skov3 cells with DF (double fusion) reporter gene. (A) Representative FACS results during GFP-signal-gated cell sorting. (B) Fluorescence microscope imaging of Skov3 (DF) cells. (C) Representative bioluminescence images of Skov3 (DF) cells, and (D) increased signals correlated with cell numbers.

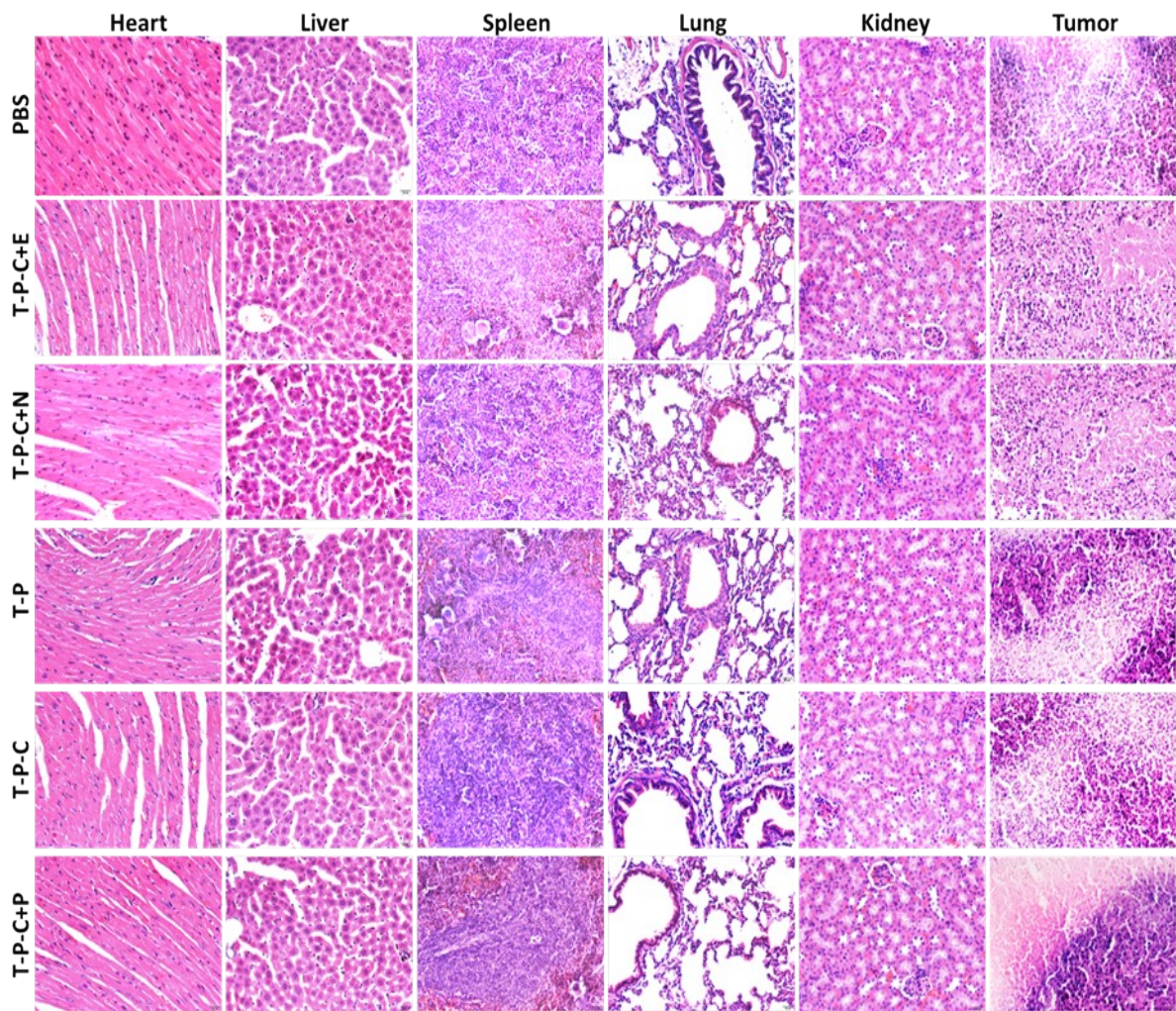


**Fig. S9** H&E staining of hearts, livers, spleens, lungs, kidneys and tumor tissues from mice treated under various conditions. T-P-C+E: Tat-TF-C16TAB+EIPA. T-P-C+N: Tat-TF-C16TAB+NAV-2729. T-P: Tat-TF. T-P-C: Tat-TF-C16TAB. T-P-C+P: Tat-TF-C16TAB+PTX. Scale bar: 50  $\mu$ m.